GMR
The Original

FABRICATION OF MULTISCALE POLYMERIC NANOSCAFFOLDS LOADED WITH GREEN SYNTHESIZED CuO NANOPARTICLES FROM *Padina tetrastromatica* EXTRACT FOR ENHANCED ANTIMICROBIAL ACTIVITY

Vishal Suraj Ravindran[1], Manodhar Naidu Vunnam[2], Ramganesh Selvarajan[3]*

[1]Saveetha Medical College & Hospital (SMCH), Saveetha Institute of Medical and Technical Sciences (SIMATS), Thandalam, Chennai, Tamil Nadu 602105, India. klssvishal@gmail.com
[2]Department of Nephrology, Saveetha Medical College and Hospital, Saveetha Institute of Medical And Technical Sciences (SIMATS), Thandalam, Chennai-602105, Tamil Nadu, India. Email: manodharnaidu9@gmail.com
[3]Centre for Microbial Ecology and Translational Research, Department of Microbiology, Saveetha Medical College and Hospital, Saveetha Institute of Medical And Technical Sciences (SIMATS), Thandalam, Chennai-602105, Tamil Nadu, India.
Email: ramganesh.presidency@gmail.com
*Corresponding Author: ramganesh.presidency@gmail.com (R.S.)

ABSTRACT
This study developed an eco-friendly approach for synthesizing copper oxide nanoparticles (CuO NPs) using *Padina tetrastromatica* brown algae extract and incorporated them into starch/polyvinyl alcohol (PVA) electrospun nanoscaffolds for antimicrobial applications. The green-synthesized CuO NPs exhibited a characteristic surface plasmon resonance peak at 273 nm (UV-Vis), while Fourier-transform infrared spectroscopy (FTIR) confirmed Cu-O bonding (602.84 cm^{-1}, 433.39 cm^{-1}) and scaffold functional groups (e.g., O-H, C-O-C). X-ray diffraction (XRD) revealed monoclinic tenorite phase CuO NPs (JCPDS 05-0661) embedded in semi-crystalline scaffolds (17.1% crystallinity). Scanning electron microscopy (SEM) showed uniform, porous nanofibers (diameter ~108 nm) with well-dispersed NPs, and Thermogravimetric analysis (TGA) indicated thermal stability up to 300°C. The nanoscaffolds demonstrated superior antimicrobial activity against Gram-negative (*Escherichia coli*: 31±0.32 mm; *Klebsiella pneumoniae*: 28±0.13 mm), Gram-positive (*Staphylococcus aureus*: 26±0.26 mm), and fungal pathogens (*Aspergillus niger*: 24±0.28 mm), outperforming individual components (extract, CuO NPs) and nearing standard drug efficacy (ciprofloxacin, voriconazole). The synergistic effects of CuO NPs and the polymer matrix highlight the scaffold's potential as a biodegradable, broad-spectrum antimicrobial material for wound dressings and tissue engineering. This study underscores the viability of algal-mediated green synthesis in developing sustainable biomedical nanocomposites.

KEYWORDS: *Padina tetrastromatica*, Green synthesis, CuO NPs, Starch/PVA nanoscaffolds, Antimicrobial activity.

1. INTRODUCTION
The rapid emergence of multidrug-resistant (MDR) pathogens has escalated the global demand for novel antimicrobial agents and advanced biomaterials, prompting a paradigm shift towards nanotechnology-based solutions in the biomedical sector [1]. Among various nanomaterials, metal oxide nanoparticles have gained considerable attention due to their unique physicochemical properties, high surface-area-to-volume ratio, and broad-spectrum antimicrobial activities [2]. Copper oxide nanoparticles (CuO NPs), in particular, have emerged as promising antimicrobial agents owing to their redox potential, catalytic efficiency, and affordability [3]. CuO NPs possess inherent biological activity and can effectively inhibit bacterial and fungal pathogens by generating reactive oxygen species (ROS), disrupting microbial membranes, and interfering with cellular metabolism [4]. However, conventional synthesis methods for CuO NPs often involve toxic chemicals and energy-intensive procedures, raising concerns regarding environmental sustainability and biomedical safety [5].
To address these challenges, green synthesis approaches utilizing plant and algal extracts have gained momentum as eco-friendly, cost-effective, and biocompatible alternatives for nanoparticle fabrication [5]. Marine macroalgae, especially brown seaweeds such as *Padina tetrastromatica*, represent a valuable and underutilized resource in green nanotechnology [6]. These seaweeds are rich in bioactive compounds, including polysaccharides, polyphenols, terpenoids, flavonoids, and proteins, which can act as natural reducing and stabilizing agents during nanoparticle formation [7]. The utilization of *P. tetrastromatica* extract in the green synthesis of CuO NPs not only eliminates the need for hazardous reagents but also imparts biofunctional properties to the resulting nanoparticles, enhancing their biological efficacy [8]. Despite the documented medicinal value of *P. tetrastromatica*, its application in nanomaterial synthesis and antimicrobial therapy remains largely unexplored, thereby warranting further investigation [9].
In recent years, the integration of nanoparticles into biodegradable polymeric matrices has gained significant interest in tissue engineering, wound healing, and antimicrobial applications [10]. Natural biopolymers such as

starch and synthetic biocompatible polymers like polyvinyl alcohol (PVA) offer excellent film-forming capabilities, hydrophilicity, and biodegradability, making them ideal candidates for scaffold fabrication [11]. Electrospinning has emerged as a powerful technique for producing nanofibrous scaffolds that mimic the extracellular matrix (ECM), promoting cell attachment, proliferation, and tissue regeneration [12]. The incorporation of metal oxide nanoparticles into electrospun nanofibers not only enhances the mechanical and thermal properties of the scaffolds but also endows them with potent antimicrobial functionality, crucial for preventing infections in wound sites and implanted biomaterials [13].

Despite these advantages, limited research has focused on developing nanofibrous composites that synergistically combine green-synthesized CuO NPs with starch/PVA matrices [14]. Such hybrid systems hold immense potential in biomedical applications, especially in fabricating antimicrobial wound dressings, drug delivery systems, and tissue engineering scaffolds0020[15]. Furthermore, comprehensive characterization of the physicochemical, thermal, structural, and biological properties of these nanocomposites is essential to ensure their functionality, safety, and effectiveness [16]. Key techniques such as UV–visible spectroscopy, Fourier-transform infrared spectroscopy (FTIR), X-ray diffraction (XRD), scanning electron microscopy (SEM), thermogravimetric analysis (TGA), and zeta potential analysis provide crucial insights into nanoparticle formation, scaffold morphology, stability, and interaction mechanisms [17].

The current study aims to address the critical need for environmentally benign and biologically potent nanomaterials by synthesizing CuO NPs using *P. tetrastromatica* extract through a green synthesis approach and incorporating them into starch/PVA-based electrospun nanofibrous scaffolds. This study encompasses a systematic investigation of the synthesized nanoparticles and composite scaffolds using advanced characterization techniques to evaluate their structural integrity, thermal stability, particle size distribution, and colloidal properties [18]. Moreover, the antimicrobial efficacy of the individual components (algal extract and CuO NPs) and the final nanofibrous scaffold was assessed against a panel of clinically relevant bacterial and fungal pathogens to establish their potential as broad-spectrum antimicrobial agents [19].

In this context, the novelty of the present research lies in its multidisciplinary approach, combining marine biotechnology, green nanotechnology, polymer science, and microbiology to develop a functional biomaterial platform [20]. Unlike conventional CuO NP synthesis methods, the use of *P. tetrastromatica* offers a sustainable and biologically enriched route to nanoparticle fabrication [3]. The integration of these nanoparticles into starch/PVA electrospun scaffolds not only enhances their antimicrobial potential but also aligns with the growing demand for biodegradable and biocompatible materials in clinical settings [21]. Importantly, this work adds new insights into the structure–function relationship of green-synthesized metal oxide nanoparticles embedded in polymeric networks and their synergistic role in microbial inhibition.

The objective of this study is to (i) synthesize CuO NPs using *P. tetrastromatica* extract through a green chemistry route, (ii) incorporate the nanoparticles into electrospun starch/PVA nanofibrous scaffolds, (iii) perform a detailed physicochemical characterization of the developed nanomaterials, and (iv) evaluate their antimicrobial activity against a range of Gram-positive, Gram-negative, and fungal pathogens. The outcomes of this research are anticipated to contribute to the development of next-generation antimicrobial scaffolds that are environmentally sustainable, biologically active, and clinically relevant for diverse biomedical applications.

2. MATERIALS AND METHODS

2.1. Materials

The green synthesis of CuO NPs was carried out using *P. tetrastromatica* seaweed, collected from the coastal region of Rameswaram, Tamil Nadu, India. Copper(II) sulfate pentahydrate ($CuSO_4 \cdot 5H_2O$, Sigma-Aldrich) served as the metallic precursor. For electrospinning, PVA (molecular weight ~115,000) acted as the base polymer, supplemented with commercial starch to improve scaffold properties. All reagents, including ethanol and Milli-Q water (Merck, Sigma-Aldrich), were of analytical grade. A HOLMARC HO-NFES-040 electrospinning unit equipped with a syringe pump was used for nanofiber fabrication.

2.2. Marine macroalgae collection

Fresh *P. tetrastromatica* was obtained from the coastal region of Rameswaram. The collected *Padina tetrastromatica* was taxonomically identified and authenticated by Dr V. Veeragurunathan, CSIR-CSMCRI-Marine Algal Research Station, Mandapam Camp 623519, Tamil Nadu, India. A voucher specimen was prepared and deposited at the Herbarium of the CSIR-CSMCRI-Marine Algal Research Station, under the accession number: SI–2025–RMM–015. This authentication ensures botanical accuracy and standardization of the study material. The specimens were initially cleaned with tap water to eliminate visible contaminants and then rinsed thoroughly with distilled water. Around 100 g of the algae were chopped, air-dried at ambient temperature for two weeks, and finally ground into a fine powder using a mechanical grinder for subsequent experimental use.

2.3. Ultrasonic-assisted extraction of bioactive compounds

To extract bioactive constituents, 2 g of the dried and powdered *P. tetrastromatica* was dispersed in 50 mL of Milli-Q water. This mixture underwent ultrasonic-assisted extraction using a LABQUEST ultrasonic cleaner (Borosil; Serial No. 941032329018) maintained at 60°C for 45 minutes. The sonication enhanced cell wall disruption, promoting the release of intracellular compounds into the aqueous solution. Post-extraction, the

solution was allowed to cool and filtered through sterile Whatman No. 1 filter paper. The clear extract was either used immediately or freeze-dried for long-term storage in airtight containers under sterile conditions [22, 23].

2.4. Green synthesis of CuO NPs

To synthesize CuO NPs, 10 mL of P. extract (prepared by dissolving 10 mg of freeze-dried powder in 10 mL of Milli-Q water) was mixed with 50 mL of 0.1 M copper sulfate pentahydrate solution, keeping a 5:1 ratio. The mixture was stirred magnetically at 650 rpm and maintained at 60°C for 2 hours. A visible change in color from blue to bluish-green indicated nanoparticle formation through Cu^{2+} ion reduction. The solution was centrifuged, and the resulting precipitate was rinsed three times with double-distilled water. The purified nanoparticles were then freeze-dried for 48 hours and stored in a desiccator for further use [24].

2.5. Electrospinning of CuO-embedded starch/PVA nanofibrous scaffolds

Electrospun nanofibrous scaffolds containing CuO NPs were fabricated by dissolving 15% (w/w) PVA in Milli-Q water under continuous stirring until fully dissolved. To this, 100 mg of starch and 100 mg of CuO NPs were added and stirred vigorously at 50°C for 2.5 hours. The homogeneous mixture was loaded into a syringe fitted with a 0.84 mm internal diameter needle and placed on a HOLMARC HO-NFES-040 electrospinning unit. Parameters were set at 11.5 kV voltage, 12.3 cm needle-to-collector distance, and 0.4 mL/h flow rate. Electrospinning continued for 6–8 hours, resulting in uniform nanofibrous mats, which were carefully collected and stored in a desiccator [25-27].

2.6. Physicochemical characterization of nanoparticles and scaffolds

2.6.1. UV-visible spectroscopy

The optical characteristics of CuO NPs and algal extract were analyzed using a VIS SPEC V-730 spectrophotometer over a wavelength range of 200 to 800 nm, using deionized water as a blank. Distinct peaks, indicative of surface plasmon resonance (SPR), confirmed nanoparticle formation. [28]

2.6.2. FTIR spectroscopy analysis

FTIR analysis (ATR mode) using a PerkinElmer Spectrum Two instrument identified functional groups in CuO NPs and CuO-integrated scaffolds. Scans were taken between 4000 and 400 cm^{-1} at 4 cm^{-1} resolution, with 64 scans per sample. Peaks representing hydroxyl, phenolic, carboxylic, and metal-oxygen groups were observed [29].

2.6.3. XRD analysis

Crystallographic studies were done using a Bruker D8 Advance XRD with CuKα radiation (λ = 1.5406 Å), at 40 kV and 40 mA. Scans ranged from $2\theta = 5°$ to 90° at a 0.029649° step size. The resulting patterns were matched with JCPDS files to validate CuO phases [30].

2.6.4. SEM analysis

Morphological assessments were carried out via SEM (JEOL JSM-IT800 NANO) after gold sputter-coating. SEM images revealed fiber morphology, nanoparticle dispersion, and scaffold porosity [31].

2.6.5. TGA

Thermal stability of the nanoscaffolds was examined using a PerkinElmer TGA 8000. Samples (~5 mg) were heated from room temperature to 550°C at a 15°C/min ramp under nitrogen. Thermograms depicted degradation stages and residual weight [32].

2.6.6. Zeta potential and particle size distribution

The Malvern Zetasizer Ultra assessed nanoparticle size and zeta potential. High absolute zeta potential values indicated enhanced colloidal stability and dispersion in aqueous solutions [29].

All data and corresponding spectra are publicly accessible in the Mendeley Data repository under DOI: 10.17632/vf8822rd8j.1.

2.7. Antimicrobial activity analysis

The antimicrobial potential of *P. tetrastromatica* extract, CuO NPs, and starch/PVA electrospun nanoscaffolds (50 µg/mL concentration for each) was investigated against selected pathogenic strains using the standard agar well diffusion method. The study encompassed both bacterial (Gram-negative: Escherichia coli, Klebsiella pneumoniae, Citrobacter koseri; Gram-positive: Staphylococcus aureus) and fungal (Aspergillus niger, Penicillium sp.) test organisms. For bacterial assays, standardized inocula (0.5 McFarland standard, equivalent to ~1.5×10^8 CFU/mL) were uniformly spread on Mueller-Hinton agar surfaces, while fungal suspensions were plated on Sabouraud dextrose agar. Test solutions (50 µL) were introduced into 6 mm diameter wells, with ciprofloxacin and voriconazole serving as positive controls for bacterial and fungal strains respectively. Following a 30-minute pre-incubation diffusion phase, bacterial cultures were maintained at 37°C for 24 hours and fungal cultures at 28°C for 48 hours. The antimicrobial efficacy was assessed by measuring the diameter of growth inhibition zones (in millimeters) surrounding each well. To ensure methodological reliability, all experiments were conducted with triplicate samples under identical conditions [33].

2.8. Statistical analysis

The quantitative data collected during experiments were processed using SPSS (version 25.0) and GraphPad Prism (version 9.0). Mean values ± standard deviation (SD) were calculated from three independent replicates. To evaluate differences between groups, one-way ANOVA was applied, followed by Tukey's or Dunnett's post hoc tests for specific comparisons where necessary. A p-value below 0.05 was considered statistically significant. Data normality was confirmed using the Shapiro–Wilk test before ANOVA. Additionally, Pearson's correlation analysis was conducted to examine associations between variables. All statistical assessments were performed with a 95% confidence level [34].

3. RESULTS

3.1. UV–visible spectroscopy

The UV-Visible spectral analysis (Fig. 1) of *P. tetrastromatica* extract and synthesized CuO NPs was carried out using a JASCO V-730 spectrophotometer within a 200–800 nm wavelength range. The data acquisition interval was set at 1 nm with a bandwidth of 1.0 nm, using deionized water as the reference blank.

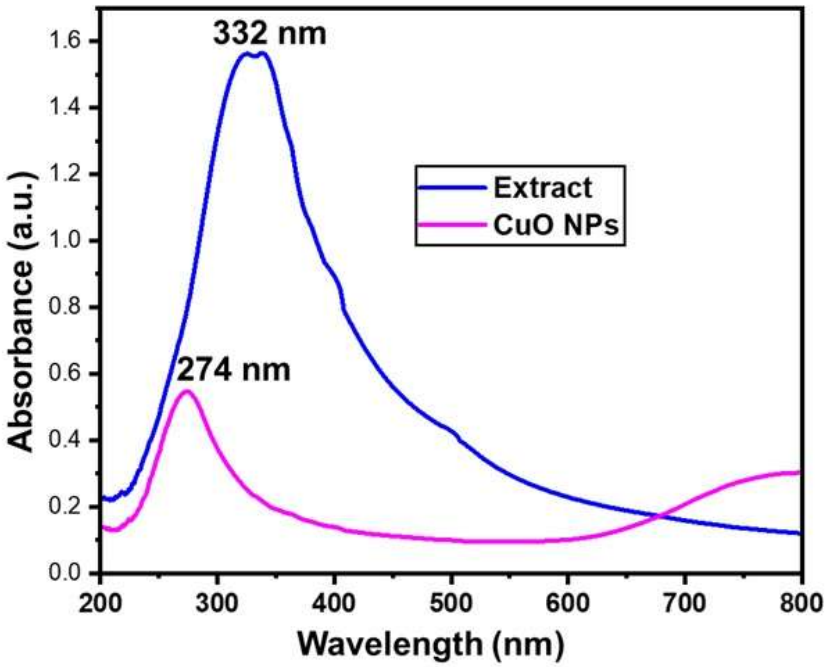

Fig. 1. UV–Visible spectral profiles of algal extract and CuO NPs.

The CuO NPs presented a pronounced absorbance peak at 273 nm with an absorbance reading of 0.547 (Fig. 1), indicative of surface plasmon resonance (SPR), confirming nanoparticle formation. Conversely, the algal extract did not show a distinct absorbance peak, indicating differing optical characteristics between the extract and nanoparticles. A scanning speed of 1000 nm/min was used, and baseline corrections were applied to enhance measurement accuracy. These spectral observations affirm the suitability of UV–Vis spectroscopy for verifying nanoparticle synthesis and assessing the optical signatures of biological and nanoparticulate samples.

3.2. FTIR spectroscopy analysis

FTIR spectra (Fig. 2) of CuO NPs and starch/PVA-based nanofibrous scaffolds were recorded using a PerkinElmer Spectrum IR system across 4000–400 cm^{-1}. The CuO NPs showed distinct vibrational bands (Fig. 2) at 602.84 cm^{-1} and 433.39 cm^{-1}, characteristic of Cu-O stretching, verifying the presence of metal-oxygen linkages. Other absorption bands at 3136.73 cm^{-1} (O-H stretch) and 1654.94 cm^{-1} (C=O stretch) suggested traces of organic moieties. For the starch/PVA scaffolds, key bands appeared at 3297.44 cm^{-1} and 3258.67 cm^{-1} (O-H stretching), 1424.21 cm^{-1} (C-H bending), and 1108.87 cm^{-1} (C-O-C stretching), indicating polysaccharide and PVA functionalities. Peaks below 1000 cm^{-1}, such as 940.79 cm^{-1} and 601.52 cm^{-1}, pointed to interactions between the polymers and CuO NPs. Overall, the spectral features confirmed the coexistence of organic functional groups and metal-oxygen bonds, establishing successful embedding of CuO into the nanofibrous matrix.

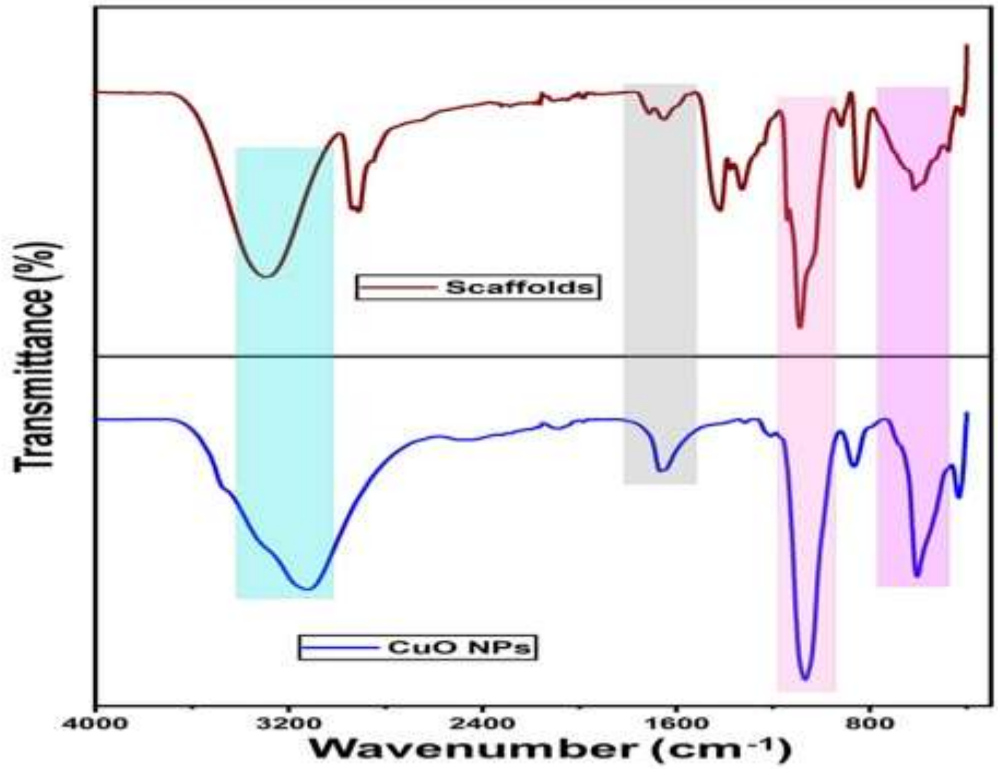

Fig. 2. FTIR spectra of CuO NPs and their incorporation into nanoscaffolds.

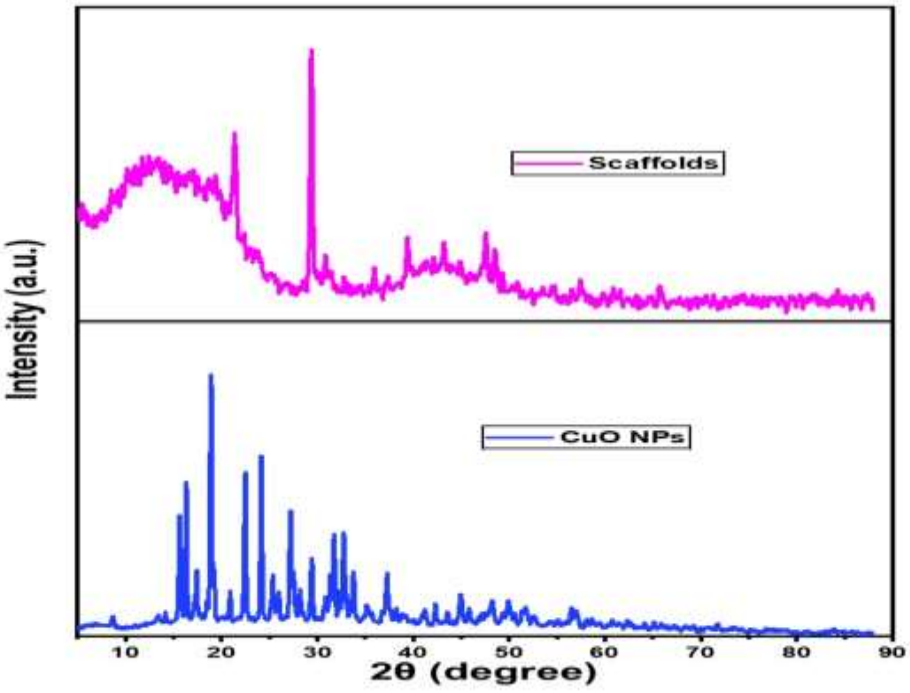

Fig. 3. XRD patterns of synthesized CuO NPs and CuO-loaded scaffolds.

3.3. XRD analysis

XRD studies (Fig. 3) of CuO NPs and starch/PVA electrospun nanoscaffolds were performed using a Bruker D8 Advance diffractometer equipped with CuKα radiation (λ = 1.5406 Å). The CuO NPs exhibited well-defined diffraction peaks at 2θ values (Fig. 3) including 13.310°, 15.601°, 16.321°, 17.433°, 18.938°, and others up to 56.302°, with d-spacings from 6.64656 Å to 1.63269 Å. The most prominent peak at 18.938° (d = 4.68228 Å, 100% intensity) indicated the monoclinic tenorite phase (JCPDS 05-0661). The starch/PVA nanoscaffold displayed semi-crystalline patterns with intense peaks at 21.307° (d = 4.16681 Å, 39.0%) and 29.349° (d = 3.04070 Å, 100%), along with minor peaks at 30.973°, 35.695°, and 39.384°, representing polymer crystallinity. The broad, lower-intensity peaks suggested an amorphous structure (82.9%) embedded with crystalline regions (17.1%),

while the distinct CuO peaks validated its high crystallinity. No impurity peaks were detected, confirming phase purity and effective incorporation of CuO into the polymer scaffold.

3.4. SEM analysis

SEM imaging (Fig. 4) of the CuO NPs and starch/PVA nanoscaffolds was conducted using a JEOL JSM-IT800 NANO microscope after gold sputter-coating to enhance conductivity. The CuO NPs appeared as spherical to slightly irregular shapes with consistent size distribution. The starch/PVA electrospun scaffolds exhibited a porous, continuous fibrous morphology with uniform fiber diameters, indicating successful electrospinning. The fibers were predominantly bead-free with smooth surfaces, and CuO NPs were visibly embedded and evenly distributed in the scaffold matrix. The open, porous three-dimensional structure facilitates cell migration and nutrient flow, supporting tissue engineering use. High-resolution images confirmed well-dispersed nanoparticles without noticeable clumping, implying strong compatibility between the polymers and CuO NPs. The observed structural attributes highlight the scaffold's potential as a biomaterial platform with desirable morphology and homogeneous nanoparticle incorporation.

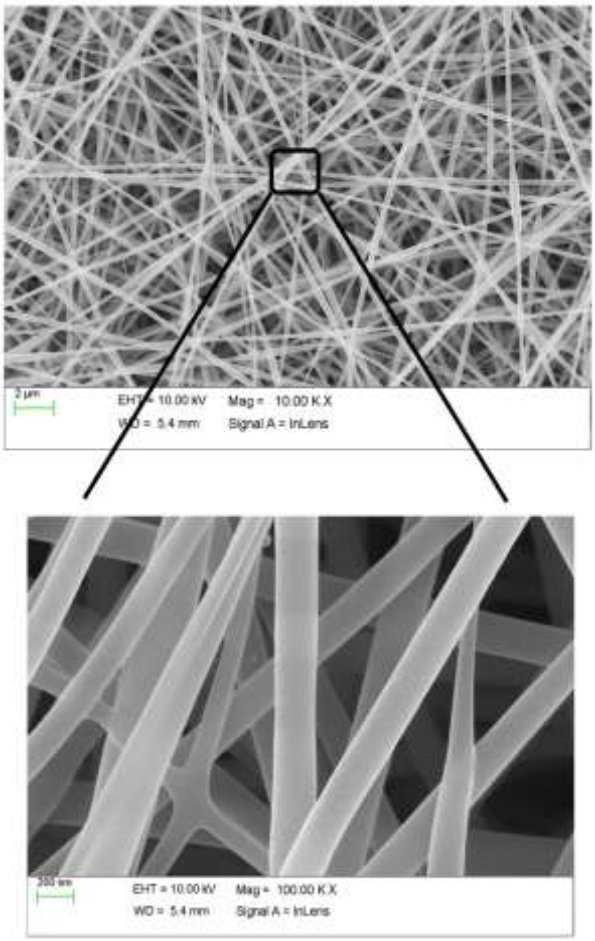

Fig. 4. SEM analysis of synthesized CuO NPs and CuO-loaded scaffolds.

3.5. TGA

Thermal degradation (Fig. 5) of starch/PVA nanoscaffolds was evaluated using a PerkinElmer TGA analyzer. A sample of 2.294 mg was subjected to heating from 30°C to 550°C at 15°C/min under a nitrogen environment (Fig. 4). A significant weight loss event was recorded beginning at 298.21°C, peaking at 356.55°C, and concluding at 395.85°C, corresponding to the breakdown of organic polymers (starch and PVA). The associated negative weight loss of -41.912% marked the decomposition of functional groups and scission of the polymer backbone. An initial minor loss below 150°C indicated moisture evaporation. The data did not include residual weight beyond 550°C, hence no inference could be drawn regarding ash or inorganic content. These thermal characteristics confirm scaffold stability up to approximately 300°C, with rapid degradation beyond, which is typical for biopolymer composites. The thermogram provides essential information on the temperature thresholds for processing and biomedical utilization of the developed nanoscaffolds.

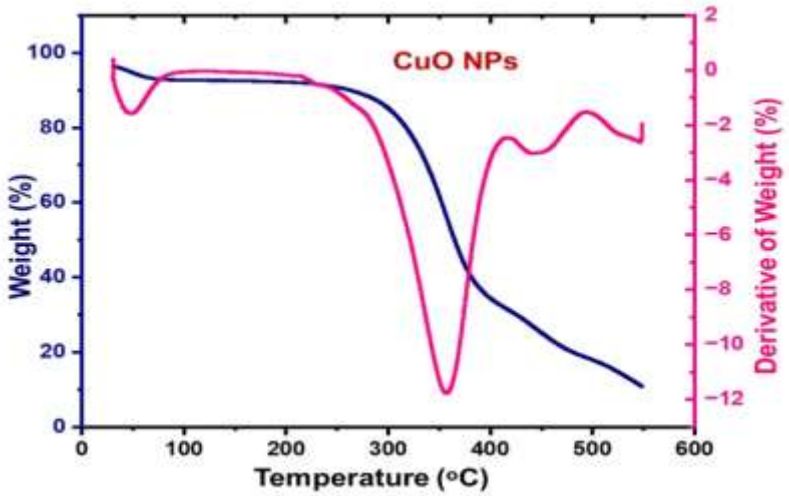

Fig. 5. Thermal degradation behavior of CuO-incorporated nanoscaffolds.

3.6. Zeta potential and particle size analysis

Dynamic light scattering (DLS) measurements for CuO NPs were performed using a Malvern Zetasizer to determine their hydrodynamic size and colloidal behavior. The size distribution analysis revealed a Z-average diameter of 108 nm (Fig. 6). Zeta potential testing showed an average surface charge of -22.13 mV, with two observable populations at -30.51 mV and -16.71 mV (Fig. 7), indicative of moderate electrostatic repulsion. The negative surface charge suggests surface-bound functional groups facilitating interparticle repulsion; however, values below ±30 mV imply a propensity for partial aggregation. Supporting data included a conductivity of 0.03211 mS/cm and a quality factor of 6.242, with derived count rates of 1570 kcps (sample) and 2163 kcps (reference). These values suggest that CuO NPs maintain a moderately stable colloidal form at 25°C, with particle size variations due to primary particles and minor aggregates. This physicochemical characterization is crucial for understanding the dispersion and interaction behavior of nanoparticles in biological systems.

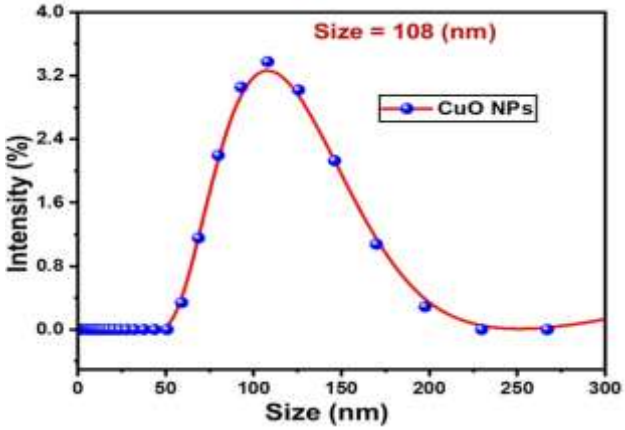

Fig.6. DLS particles size analysis of CuO NPs

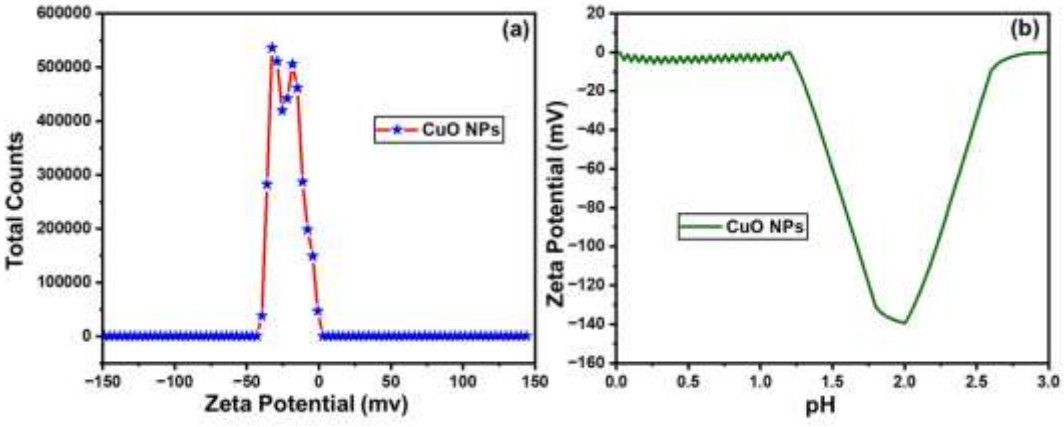

Fig.7. Zeta-potential analysis of CuO NPs

3.7. Antimicrobial evaluation

The antimicrobial evaluation of *P. tetrastromatica* extract, CuO NPs, and starch/PVA electrospun nanoscaffolds (50 µg/mL) demonstrated varying efficacy against bacterial and fungal pathogens (Table 1). The algal extract exhibited moderate antibacterial activity, with inhibition zones of 21±0.14 mm for *Escherichia coli*, 20±0.22 mm for *Klebsiella pneumoniae*, 20±0.38 mm for *Staphylococcus aureus*, and 21±0.11 mm for *Citrobacter koseri*, while showing 18±0.14 mm and 20±0.26 mm against *Aspergillus niger* and *Penicillium* sp., respectively. CuO NPs displayed stronger effects, particularly against bacteria (28±0.18 mm for *E. coli*, 25±0.17 mm for *K. pneumoniae*, 24±0.30 mm for *S. aureus*, and 25±0.13 mm for *C. koseri*) and fungi (22±0.12 mm for *A. niger*, 24±0.16 mm for *Penicillium* sp.). The nanoscaffolds outperformed both, achieving 31±0.32 mm (*E. coli*), 28±0.13 mm (*K. pneumoniae*), 26±0.26 mm (*S. aureus*), 27±0.12 mm (*C. koseri*), 24±0.28 mm (*A. niger*), and 26±0.12 mm (*Penicillium* sp.), nearing the efficacy of controls (ciprofloxacin: 28–33 mm; voriconazole: 26–28 mm). These results highlight the nanoscaffolds' superior antimicrobial potential, likely due to synergistic effects of CuO NPs and polymer matrix, while the extract and NPs alone showed intermediate activity. All tests were conducted in triplicate, ensuring reproducibility.

Table 1: Antimicrobial activity of *P. tetrastromatica* extract, CuO NPs, and starch/PVA electrospun nanoscaffolds at concentration of 50 µg/mL against various pathogenic organisms.

S. No	Organisms	Zone of inhibition (mm)				
		Ciprofloxacin (Antibiotic)	Voriconazole (Antifungal)	Algal Extract	CuO NPs	Nano-scaffolds
	Escherichia coli	33±0.58	-	21±0.14	28±0.18	31±0.32
	Klebsiella pneumoniae	30±0.14	-	20±0.22	25±0.17	28±0.13
	Staphylococcus aureus	28±0.32	-	20±0.38	24±0.30	26±0.26
	Citrobacter koseri	29±0.47	-	21±0.11	25±0.13	27±0.12
	Aspergillus niger	-	26±0.65	18±0.14	22±0.12	24±0.28
	Penicillium species	-	28±0.39	20±0.26	24±0.16	26±0.12

4. DISCUSSION

The present study comprehensively characterized CuO NPs synthesized using *P. tetrastromatica* extract and their successful incorporation into starch/PVA -based electrospun nanofibrous scaffolds. Multiple analytical techniques were employed to evaluate their physicochemical properties, thermal behavior, morphology, colloidal stability, and antimicrobial efficacy.

The UV–Visible spectroscopy results confirmed the formation of CuO NPs through the detection of a characteristic absorbance peak at 273 nm, attributed to surface plasmon resonance (SPR). This absorbance signal, which is absent in the algal extract alone, underscores the distinct optical behavior of the synthesized nanoparticles. The presence of SPR also provides indirect evidence of nanoparticle size and distribution, as it is typically associated with well-dispersed and stable nanomaterials. These findings demonstrate the utility of UV–Vis spectroscopy in preliminary nanoparticle identification and monitoring of synthesis processes [35-41].

FTIR spectroscopy further revealed the successful synthesis and stabilization of CuO NPs and their integration within the polymeric matrix. The characteristic Cu–O vibrations identified at 602.84 cm^{-1} and 433.39 cm^{-1} confirmed the formation of CuO bonds. The detection of O–H and C=O stretching vibrations indicated the presence of organic moieties from the algal extract, suggesting that biomolecules may have acted as reducing and stabilizing agents. The spectra of starch/PVA nanoscaffolds exhibited typical bands associated with polysaccharides and PVA, including O–H, C–H, and C–O–C stretches. Notably, additional peaks below 1000 cm^{-1} suggested successful interaction and embedding of CuO NPs within the scaffold matrix, validating the compatibility and integration of nanoparticles with the polymeric system [42-47].

XRD analysis provided insight into the crystalline nature of the CuO NPs and the composite scaffold. The CuO NPs exhibited sharp, intense peaks corresponding to a monoclinic tenorite phase, as confirmed by comparison with standard JCPDS data. These crystalline peaks were well preserved in the composite scaffold, indicating that the nanoparticle structure remained intact during scaffold fabrication. In contrast, the polymeric nanoscaffold displayed semi-crystalline features characterized by broad peaks, consistent with the inherent amorphous nature of starch and PVA. Quantitative analysis of the XRD pattern showed 17.1% crystallinity, with the remaining 82.9% indicating an amorphous matrix. The retention of CuO crystallinity in the scaffold, coupled with the amorphous polymer base, suggests a balanced structure capable of supporting both mechanical integrity and bioactivity [48-53].

SEM revealed essential morphological details. The CuO NPs appeared predominantly spherical with a relatively uniform size distribution, supporting earlier UV–Vis and XRD results. SEM images of the electrospun scaffolds exhibited well-formed, bead-free, continuous fibers with uniform diameters and interconnected porous architecture. These morphological characteristics are highly desirable for biomedical scaffolds, as they facilitate nutrient transport, gas exchange, and cellular migration. Furthermore, the nanoparticles were visibly and evenly dispersed throughout the scaffold without aggregation, indicating strong intermolecular interactions and

compatibility between the polymer matrix and CuO NPs. This uniform distribution is crucial for achieving consistent antimicrobial activity and biological performance across the entire scaffold surface [54-62].
TGA offered valuable data on the thermal stability of the nanofibrous scaffolds. The scaffold remained stable up to nearly 300°C, after which rapid degradation occurred due to the breakdown of starch and PVA chains. The initial weight loss below 150°C was attributed to moisture evaporation, a common phenomenon in biopolymer systems. The major degradation phase, observed between 298.21°C and 395.85°C, reflects polymer backbone decomposition. The overall thermal profile aligns with typical behavior of biopolymer composites, reaffirming the scaffold's suitability for biomedical applications that do not require high thermal resistance. The TGA results also support the scaffold's processing and storage under physiological or slightly elevated temperatures without compromising structural integrity [63-69].
DLS and zeta potential analysis provided insight into the colloidal behavior and surface chemistry of the synthesized CuO NPs. A Z-average particle diameter of 108 nm places the particles within the nanometric range ideal for biological interactions, including cellular uptake and antimicrobial action. The zeta potential value of -22.13 mV indicates moderate stability in aqueous suspension, with some propensity for aggregation due to values falling slightly below the ±30 mV threshold generally associated with high colloidal stability. The presence of negative surface charge, derived from functional groups on the nanoparticle surface, contributes to electrostatic repulsion and inhibits rapid aggregation. These data emphasize the importance of surface chemistry in maintaining nanoparticle dispersion and functional behavior in biological environments [70-74].
The antimicrobial activity evaluation clearly demonstrated the enhanced bioefficacy of the CuO-loaded starch/PVA nanoscaffolds. While the *P. tetrastromatica* extract exhibited moderate inhibitory effects, and the CuO NPs showed stronger antibacterial and antifungal activity, the composite nanoscaffolds surpassed both in performance. The larger zones of inhibition observed for the nanoscaffolds against all tested pathogens—*Escherichia coli*, *Klebsiella pneumoniae*, *Staphylococcus aureus*, *Citrobacter koseri*, *Aspergillus niger*, and *Penicillium* sp.—reflect a synergistic effect between the CuO NPs and the biopolymer matrix. This enhanced efficacy is likely due to the improved release kinetics and localized concentration of CuO within the scaffold structure, combined with the inherent biocompatibility and hydrophilicity of starch/PVA. Compared with standard antimicrobial agents such as ciprofloxacin and voriconazole, the scaffolds showed near-comparable activity, positioning them as promising alternatives for antimicrobial wound dressing and tissue engineering applications [75-77].
The comprehensive characterization of CuO NPs and their successful incorporation into starch/PVA electrospun scaffolds establishes a multifunctional platform with favorable physicochemical properties, thermal resilience, and broad-spectrum antimicrobial potential. These findings support the continued development of such nanocomposites for biomedical use, particularly in wound healing and infection control.

5. CONCLUSION

This study successfully demonstrated the green synthesis of CuO NPs using *P. tetrastromatica* extract and their effective incorporation into starch/PVA electrospun nanoscaffolds for antimicrobial applications. The nanoparticles exhibited characteristic physicochemical properties, including a distinct SPR peak (273 nm), Cu-O vibrational bonds (FTIR), and monoclinic crystallinity (XRD). The nanoscaffolds displayed a porous, fibrous morphology (SEM) with uniform NPs dispersion and thermal stability up to 300°C (TGA). Antimicrobial assays revealed superior efficacy of the composite scaffolds, with inhibition zones of 31±0.32 mm (*E. coli*), 28±0.13 mm (*K. pneumoniae*), and 24±0.28 mm (*A. niger*), outperforming standalone algal extract or CuO NPs. The synergistic interaction between CuO NPs and the polymer matrix enhanced antimicrobial activity, nearing the potency of conventional drugs. These findings highlight the scaffold's potential as a sustainable, broad-spectrum antimicrobial material for wound healing and tissue engineering. The eco-friendly synthesis approach and robust biological performance position this nanocomposite as a promising alternative to conventional antimicrobial agents, addressing both environmental and biomedical challenges.

Ethics declaration: Not Applicable

Conflicts of Interest: The authors declare no conflicts of interest.

Data Availability Statement: The full dataset of physiochemical characterization associated with this work is published in Mendeley Data [Dataset] Padina tetrastromatica-driven synthesis meets biopolymers: comprehensive profiling of starch nanoscaffolds infused with eco-friendly copper oxide nanoparticles (DOI: 10.17632/ddbgcpm32x.1). Disclosure: The material characterization data and figures (e.g., UV, SEM, FTIR, XRD, TGA, Zeta Potential and particle sizer) presented here were generated from a common dataset and are being reused across multiple related studies on nanomaterials. All biological analyses and conclusions are original to each manuscript.

REFERENCES

[1] Natarajan PM, Swamikannu B, Sivaraman NM, Stylin AGSQ. Prevention of Oral Cancer: A Comprehensive Guide. Journal of Pharmacy and Bioallied Sciences. 2024; 16(5): S4239-S4241.

[2] Umapathy V, Dhanavel A, Kesavan R, Natarajan PM, Bhuminathan S, Vijayalakshmi P. Anticancer Potential of the Principal Constituent of Piper nigrum, Piperine: A Comprehensive Review. Cureus. 2024; 16(2): e54425.
[3] Umapathy VR, Swamikannu B, Natarajan PM, Devi R, Nandini MS, Vimalarani, Vijayalakshmi P. In Silico Molecular Docking of Ocimum sanctum Phytochemicals: Targeting Key Biomarkers in Oral Cancer. Journal of Pharmacy and Bioallied Sciences. 2024; 16(5): S4792-S4799.
[4] Natarajan PM, Bhuminathan S, Rajan R, Bindu K, Loganathan K, Veerakumar R. The Crucial Role of Smoking Cessation in Preventing Oral Cancer. Journal of Pharmacy and Bioallied Sciences. 2024; 16(5): S4245-S4247.
[5] Swamikannu B, Umapathy VR, Natarajan PM, Nandini MS, Stylin AGSQ, Vimalarani V, Rajinikanth S. Unlocking the Therapeutic Benefits of Artemisia Annua: A Comprehensive Overview of its Medicinal Properties. Journal of Pharmacy and Bioallied Sciences. 2024; 16(5): S4248-S4253.
[6] Natarajan PM. Computational Studies on Recent Congeners of Fluoroquinolones and Nitroimidazoles for Their Use in Periodontal Therapy. Journal of Pharmacy and Bioallied Sciences. 2024; 16(5): S4731-S4740.
[7] Yadalam PK, Arumuganainar D, Natarajan PM, Ardila CM. Artificial intelligence-powered prediction of AIM-2 inflammasome sequences using transformers and graph attention networks in periodontal inflammation. Scientific Reports. 2025; 15: 8733.
[8] Yadalam PK, Chatterjee S, Natarajan PM, Ardila CM. Comparison of light gradient boosting and logistic reg ression for interactomic hub genes in Porphyromonas gingivalis and Fusobacterium nucleatum-induced periodo ntitis with Alzheimer's disease. Frontiers in Oral Health. 2025; 6:1463458.
[9] Natarajan PM, Bhuminathan S, Leela B, Bindu K, Loganathan K, Ramachandran V. Smoking and its Role in Oral Cancer. Journal of Pharmacy and Bioallied Sciences 16(5): S4242-S4244.
[10] Yadalam PK, Natarajan PM, Ardila CM. Variational graph autoencoder for reconstructed transcriptomic data associated with NLRP3 mediated pyroptosis in periodontitis. Scientific Reports. 2025; 15: 1962.
[11] Pei JJ, Perumal NC, Meng P, Long Q, Palanisamy CP. AI-assisted FTIR spectroscopic profiling of exosomes: Emerging frontiers in early detection of Alzheimer's disease. Ageing Research Reviews. 2026; 103311.
[12] Raja FSD, Abraham L, Rangasamy K, Saikia K, Rathankumar AK, Mironescu M, Mironescu I, Palanisamy CP, Kanniappan GV. Next-Generation Microbiome Therapeutics: Psychobiotics and Fecal Microbiota Transplants (FMT) for Mental Health Treatment. Frontiers in Cellular and Infection Microbiology. 2026; 16: 1719357.
[13] Subramani K, Srinivasan S, Shanmugam P, Palanisamy CP, Sonsudin F, Poompradub S. Sustainable phytochemical mediated-ZnO nanoparticles derived from Crescentia cujete for toxicological evaluation and multifunctional environmental applications. Environmental Nanotechnology, Monitoring & Management. 2026; 26: 101180.
[14] Kunamalla RP, Panagal M, Palanisamy CP. Green-engineered multiscale starch/PVA nanofibrous scaffolds embedded with CuO nanoparticles from Sargassum ilicifolium for potent antimicrobial performance. Genetics and Molecular Research. 2026; 25(13s): 1-9.
[15] Dharmaprakash S, Gunasekaran VP, Sivaramakrishnan R, Kanniappan GV, Jayaraman S, Mironescu M, Rajabathar JR, Mironescu ID, Palanisamy CP. Marine macroalgae-mediated ultrasonic-assisted green synthesis of CuO nanoparticles embedded in starch/PVA electrospun nanoscaffolds for in vitro α-amylase and α-glucosidase inhibitory activity. Scientific Reports. 2026; 16: 26243.
[16] Surendran N, Chandrasekaran G, Raju MV, Chandrasekaran MK, Ahalliya RM, Palanisamy CP, Kanniappan GV, Arcot R, Alharbi NS, Thiruvengadam M. Anti-inflammatory potential of ethanolic extract of Maranta arundinacea L.: Insights from COX-2 modulation and oxidative stress analysis. South African Journal of Botany. 2026; 195: 142-151.
[17] Pei J, Senthilkumar MV, Hessini K, Subramaniyam S, Sivaramakrishnan R, Kanniappan GV, Jayaraman S, Palanisamy CP. Green fabrication of starch/PVA/CuO nanoscaffolds using marine macroalgae extract for enhanced anti-inflammatory activity. Sustainable Chemistry and Pharmacy. 2026; 51: 102397.
[18] Balasubramanian V, Loganathan L, Muthuswamy K, Viswanathan TM, Raju MV, Chandrasekaran MK, Ahalliya RM, Poorasamy J, Palanisamy CP, Dominic S, Kanniappan GV. Anticancer therapeutic efficacy of PEGylated β-galactosidase from Aspergillus terreus in DMBA-induced breast cancer: Toxicological, molecular and histopathological evaluation in Wistar rats. International Journal of Biological Macromolecules. 2026; 360: 151856.
[19] Jayaraman S, Eswaran A, Rajagopal P, Palanisamy CP, Veerakumar P, Veeraraghavan VP, Sirasanagandla SR. Neuroendocrine-associated epigenetic factors in cellular senescence: mechanisms and therapeutic implications. Biogerontology. 2026; 27(2): 64.
[20] Ponnusamy B, Rajagopal P, Palanisamy CP, Veeraraghavan VP, Jayaraman S. Mechanistic Exploration of the anticancer activity of Justicia adhatoda Plant Leaf Ethanolic Extract against Colon Cancer Cells: An in silico and in vitro Approach. Asian Pacific Journal of Cancer Prevention. 2026; 27(3): 1069-1080.
[21] Pei J, Saran VS, Sivaramakrishnan R, Kanniappan GV, Pandurangan V, Jayaraman S, Dhayalan VK, Mironescu M, Mironescu ID, Palanisamy CP. Ultrasonic-assisted, Sargassum ilicifolium (brown marine macroalgae)-mediated biogenic synthesis of CuO nanoparticles incorporated in starch/PVA electrospun nanoscaffolds: In vitro safety and antioxidant efficacy assessment. Bioorganic Chemistry. 2026; 173: 109679.

[22] Raj MAPA, Subramaniyam S, Kanniappan GV, Jayaraman S, Palanisamy CP. Sustainable fabrication of starch/PVA/CuO electrospun nanoscaffolds from Turbinaria ornata (marine macroalgae) extract: Physicochemical characterization and antidiabetic evaluation. Kuwait Journal of Science. 2026; 53(2): 100545.
[23] Pei J, Ganesh NS, Subramaniyam S, Sivaramakrishnan R, Kanniappan GV, Jayaraman S, Palanisamy CP. Sustainable fabrication of starch/PVA/CuO electrospun nanoscaffolds from Padina tetrastromatica (Brown macroalgae) extract: Physicochemical characterization and antidiabetic assessment. Sustainable Chemistry One World. 2026; 9: 100195.
[24] Sakthiraj A, Sivaramakrishnan R, Subramaniyam S, Kanniappan GV, Pandurangan V, Jayaraman S, Dhayalan VK, Mironescu M, Mironescu ID, Palanisamy CP. Starch/PVA electrospun nanoscaffolds loaded with ultrasonic-assisted green-synthesis of CuO nanoparticles from marine macroalgae (Gracilaria corticata) extract: Cytotoxicity and antioxidant analysis. Chemical Physics Impact. 2026; 12: 101018.
[25] Raju M, Chandrasekaran MK, Loganathan L, Ahalliya RM, Mironescu M, Mironescu ID, Palanisamy CP, Kanniappan GV. Lipid remodeling and ferroptosis in phosphatidylcholine-mediated tumor–stroma crosstalk. Frontiers in Molecular Biosciences. 2026; 13: 1742305.
[26] Kunamalla R, Panagal M, Palanisamy CP. Biogenic synthesis and fabrication of starch/PVA/CuO electrospun nanoscaffolds from Sargassum ilicifolium (brown marine macroalgae) extract for anticancer activity on HT-29 and MCF-7 cancer cells. Biocatalysis and Agricultural Biotechnology. 2026; 72: 103923.
[27] Pei J, Govindaraj H, Sivaramakrishnan R, Kanniappan GV, Pandurangan V, Dhayalan VK, Mironescu M, Mironescu ID, Jayaraman S, Palanisamy PC. Sustainable fabrication of biopolymer-based (starch/PVA) nanoscaffolds loaded with green-synthesized CuO nanoparticles from Sargassum wightii (marine macroalgae): Cytocompatibility and antioxidant activity. Biomaterials Advances. 2026; 182: 214660.
[28] Pei J, Perumal NC, Meng P, Long Q, Palanisamy CP. Extracellular vesicle-based biosensors for Alzheimer's disease: A new frontier in precision diagnostics. Ageing Research Reviews. 2026; 113: 102904.
[29] Shree P, Sivaramakrishnan R, Kanniappan GV, Pandurangan V, Jayaraman S, Dhayalan VK, Mironescu M, Mironescu ID, Palanisamy CP. Antioxidant and biocompatible CuO-starch/PVA nanoscaffolds via ultrasonic green synthesis using Turbinaria conoides (brown marine macroalgae). Medicine in Drug Discovery. 2025; 28: 100238.
[30] Gong J, Lin J, Guan T, Pei J, Palanisamy CP, El-AtyFrom AMA. selenium tolerance to nanoplastic antagonism: Comprehensive characterization of L. casei SNUT1 and its extracellular vesicle–nanoselenium complex. Food Bioscience. 2025; 74: 107749.
[31] Poochi SP, Sundarraj R, Raju MV, Chandrasekaran MK, Ahalliya RM, Palanisamy CP, Kanniappan GV, Kondapavuluri BK, Thiruvengadam M. Harnessing Nature: Computational and Experimental Insights Into *Ipomoea obscura* Metabolites for Bladder Cancer Therapy. Chemistry and Biodiversity. 2025; 0: e00909.
[32] Dugganaboyana GK, Kannankumar MKG, Shivaramakrishna S, Raju MV, Chandrasekaran MK, Ahalliya RM, Panneerselvam N, Palanisamy CP, Kanniappan GV. Phytochemical insights, antioxidant activity and therapeutic potential of Cassia senna against prostate cancer in Wistar albino rats. Discover Applied Sciences. 2025; 7:1206.
[33] Natarajan SR, Krishnamoorthy R, Alshuniaber MA, Gatasheh MK, Rajagopal P, Veeraraghavan VP, Palanisamy CP, Jayaraman S. KDM1A Facilitates Oncogenic Potential in Colorectal Cancer Progression Through the Activation of AXIN/GSK3β/β-Catenin Signaling Pathways: Evidence From Integrated Transcriptomics and In Vitro Studies. The Journal of Gene Medicine. 2025; 27(11): e70053.
[34] Guan T, Gong J, Lin J, Palanisamy CP, Jinjin Pei J, El-Aty AMA. Machine learning-driven multimodal optimization of selenium biotransformation and flavor profiling in fermented apple–Yacon functional beverages. Innovative Food Science & Emerging Technologies. 2025; 105: 104198.
[35] Natarajan SR, Krishnamoorthy R, Alshuniaber MA, Alsulami TS, Gatasheh MK, Rajagopal P, Palanisamy CP, Govindan R, Veeraraghavan VP, Jayaraman S. ABCE1 facilitates tumour progression via aerobic glycolysis and inhibits cell death in human colorectal cancer cells through the p53 signalling pathway. Scientific Reports. 2025; 15: 24674.
[36] Huang Y, Guo H, Liu Y, Jin W, Palanisamy CP, Pei J, Oz F, El-Aty AMA. Effects of Natural Polysaccharides on the Gut Microbiota Related to Human Metabolic Health. Molecular Nutrition & Food Research. 2025; 69:e202400792.
[37] Poornima K, Meenakshi K.C, Manikandan V.R, Shankari G, Prabhu D, Rathi M.A, Palanisamy CP, Balaji R, Gopalakrishnan V.K. Exploring the anticancer potential of Jerantinine A from *Tabernaemontana coronaria* against prostate, breast, and ovarian cancers: A computational approach. *Journal of Complementary and Integrative Medicine*, 2025 22(2): 363–372.
[38] Palanisamy CP, Poompradub S, Sansanaphongpricha K, Jayaraman S, Subramani K. Faridah Sonsudin gGreen synthesis of Nigella sativa-mediated silver nanoparticles for enhanced antibacterial activity and wound healing: Mechanistic insights and biomedical applications. Environmental Nanotechnology, Monitoring & Management. 2025; 24: 101085.
[39] Surendran N, Raju MV, Chandrasekaran MK, Ahalliya RM, Palanisamy CP, Chandrasekaran G, Kanniappan GV. Physicochemical characterization of starch from Maranta arundinacea L.(arrowroot) rhizomes and its inhibition of COX-2: In vivo validation. Bioactive Carbohydrates and Dietary Fibre. 2025; 33: 100465.

[40] Kannappan P, Chandrasekaran MK, Raju MV, Gopalakrishnan S, Dhamodharan P, Ahalliya RM, Palanisamy CP, Raju B, Kanniappan GV. Exploring the anticancer potential of Jerantinine A from Tabernaemontana coronaria against prostate, breast, and ovarian cancers: a computational approach. Journal of Complementary and Integrative Medicine. 2025; 22(02): 363-372.
[41] Pei J, Kumarasamy RV, Jayaraman S, Kanniappan GV, Long Q, Palanisamy CP. Quercetin-functionalized nanomaterials: Innovative therapeutic avenues for Alzheimer's disease management. Ageing Research Reviews. 2025; 104: 102665.
[42] Jayaraman S, Prasad M, Natarajan SR, Krishnamoorthy R, Alshuniaber MA, Gatasheh MK, Veeraraghavan VP, Rajagopal P, Palanisamy CP. Molecular mechanisms underlying the effects of beta-sitosterol on TGF-β1/Nrf2/SIRT1/p53-mediated signaling in the kidney of a high-fat diet and sucrose-induced type-2 diabetic rat. Chemico-Biological Interactions. 2025; 411: 111443.
[43] Huang Y, Guo H, Liu Y, Jin W, Palanisamy CP, Pei J, Oz F, El-Aty AMA. Effects of Natural Polysaccharides on the Gut Microbiota Related to Human Metabolic Health. Molecular Nutrition & Food Research. 2025; e202400792.
[44] Prabhakaran P, Palanisamy CP, Shanmugam A, Damodharan P, Swaminathan H, Devaraj D, Ahalliya RM, Kanniappan GV. Isolation, structural characterization, and molecular docking studies on the bioactive compound from n-Hexane extract of Emilia sonchifolia (L.) DC against the pancreatic cancer target Aurora 2 Kinase. Journal of Complementary and Integrative Medicine. 2024; 22(1): 0290.
[45] Jiang H, Kumarasamy RV, Pei J, Raju K, Kanniappan GV, Palanisamy CP. Integrating engineered nanomaterials with extracellular vesicles: Advancing targeted drug delivery and biomedical applications. Frontiers in Nanotechnology. 2024; 6: 1513683.
[46] Guo H, Liu Y, Wan T, Song D, Palanisamy CP, Geng J, Pei J, Özmen S, El-Aty AMA. Toward personalized cancer management: Role of precision nutrition–diet interventions. Journal of Functional Foods. 2024; 123: 106584.
[47] Natarajan SR, Krishnamoorthy R, Alshuniaber MA, Al-Anazi KM, Farah MA, Rajagopal P, Palanisamy CP, Veeraraghavan VP, Jayaraman S. Identification of FOXM1 as a novel protein biomarker and therapeutic target for colorectal cancer progression: Evidence from immune infiltration and bioinformatic analyses. International Journal of Biological Macromolecules. 282 (Part 4): 137201.
[48] Rajendran MS, Jayaraman S, Khan JM, Jasmine S, Prabhakaran RK, Raju MV, Chandrasekaran MK, Ahalliya RM, Kannappan P, Palanisamy CP, Kanniappan GV. Investigating the colon toxicity and carcinogenic role of monosodium glutamate compared with Dimethylhydrazine in male Wistar rats: Exploring the link to childhood colon cancer risk. Journal of King Saud University - Science. 2024; 36(11): 103507.
[49] Kumarasamy RV, Natarajan P, Umapathy VR, Roy JR, Rab SO, Saeed M, Panagal M, Mironescu M, Srinivasan GP, Palanisamy CP. Clinical Applications and Therapeutic Potentials of Advanced Nanoparticles: A Comprehensive Review on Completed Human Clinical Trials. Frontiers in Nanotechnology. 2024; 6:1479993.
[50] Natarajan PM, Umapathy VR, Murali A, Swamikannu B. (2022). Computational Simulations of Identified marine-derived Natural Bioactive Compounds As Potential Inhibitors of Oral Cancer. Future Science OA. 2022; 8(3).
[51] Natarajan PM, Umapathy VR. Role of transcriptomics in the study of oral cancer. Frontiers in Oral Health. 2025; 6:1524364.
[52] Vidhyarekha U, Natarajan PM, Bhuminathan S, Sabarinathan J, Suba R, Vijayalakshmi P. Role of artificial intelligence in Oral Cancer. Advances in Public Health. 2024. 2024: 3664408.
[53] Ganesan A, Kumar NG, Natarajan PM, Gauthaman J. Automated classification of elongated styloid processes using deep learning models-an artificial intelligence diagnostics. Frontiers in Oral Health. 2025; 5: 1424840.
[54] Umapathy VR, Natarajan PM, Swamikannu B. Regenerative Strategies in Dentistry: Harnessing Stem Cells, Biomaterials and Bioactive Materials for Tissue Repair. Biomolecules. 2025; 15: 546.
[55] Natarajan PM. Dental Bioinformnatics-Current Scope and Future perspectives. Research Journal of Pharmacy and Technology. 2022;15(5):2351-6.
[56] Ganesan A, Kumar NG, Natarajan PM. Solanum trilobatum leaf extract-derived silver nanoparticles downregulate the PI3K/AKT/mTOR signaling pathway and attenuate oral squamous cell carcinoma cell proliferation. Journal of Herbmed Pharmacology. 2024; 13(2): 300-307.
[57] Perumal MKK, Renuka RR, Subbiah SK, Natarajan PM. Artificial intelligence-driven clinical decision support systems for early detection and precision therapy in oral cancer: a mini review. Frontiers in Oral Health. 2025; 6: 1592428.
[58] Ramesh E, Ganesan A, Lakshmi KC, Natarajan PM. Artificial intelligence-based diagnosis of oral leukoplakia using deep convolutional neural networks Xception and MobileNet-v2. Frontiers in Oral Health. 2025; 6: 1414524.
[59] Ganesan A, Kumar NG, Natarajan PM. Anticancer activity of silver nanoparticles synthesized from aqueous leaf extract of Solanum trilobatum (Purple fruit pea eggplant) on human oral cancer cells. Journal of Herbmed Pharmacololgy. 2024; 13(2): 260-268.

[60] Jin W, Pei JJ, Roy JR, Jayaraman S, Ahalliya RM, Kanniappan GV, Mironescu M, Palanisamy CP. Comprehensive review on single-cell RNA sequencing: A new frontier in Alzheimer's disease research. Ageing Research Reviews. 2024; 274: 102454.
[61] Pei J, Palanisamy CP, Jayaraman S, Natarajan PM, Umapathy VR, Roy JR, Panagal M, Jayaraman S. Curcumin-loaded polymeric nanomaterials as a novel therapeutic strategy for Alzheimer's disease: A comprehensive review. Ageing Research Reviews. 2024; 99: 102393.
[62] Pei J, Palanisamy CP, Jayaraman S, Natarajan PM, Umapathy VR, Roy JR, Thalamati D, Ahalliya RM, Kanniappan GV, Mironescu M. A comprehensive review on starch-based Sustainable Edible Films Loaded with Bioactive Components for Food Packaging. International Journal of Biological macromolecules. 2024; 274 (Part-1): 133332.
[63] Palanisamy CP, poompradub S, Sansanaphongpricha K, Subramani K, Sonsudin F. Increased expression levels of PDGF and VEGF magnify the wound healing potential facilitated by biogenic synthesis of silver nanoparticles. Nano-Structures & Nano-Objects. 2024; 39: 101236.
[64] Pei J, Palanisamy CP, Jayaraman S, Natarajan PM, Umapathy VR, Roy JR, Thalamati D, Ahalliya RM, Kanniappan GV, Mironescu M. Proteomics Profiling of Extracellular Vesicle for Identification of Potential Biomarkers in Alzheimer's Disease: A Comprehensive Review. Ageing Research Reviews. 2024; 99: 102359.
[65] Xi J, Wang T, Xian P, Liu X, Du M, Yang H, Palanisamy CP, Lin W, Long Q. Proteomic insights uncover enhanced neurotherapeutic potential in conditioned mesenchymal stem cell-derived extracellular vesicles. Extracellular Vesicle. 2024; 3: 100037.
[66] Pei J, Natarajan PM, Umapathy VR, Swamikannu B, Sivaraman NM, Krishnasamy L, Palanisamy CP. Advancements in the synthesis and functionalization of zinc oxide-based nanomaterials for enhanced oral cancer therapy. Molecules. 2024; 29(11): 2706.
[67] Gatasheh MK, Natarajan SR, Krishnamoorthy R, Alsulami TS, Rajagopal P, Palanisamy CP, Veeraraghavan VP, Jayaraman S. Molecular analysis to identify novel potential biomarkers as drug targets in colorectal cancer therapy: an integrated bioinformatics analysis. Molecular and Cellular Oncology. 2024; 11(1): 2326699.
[68] Pei J, Yan Y, Jayaraman S, Rajagopal P, Natarajan PM, Umapathy VR, Gopathy S, Roy JR, Sadagopan CS, Thalamati D, Palanisamy CP, Mironescu M. A review on advancements in the application of starch-based nanomaterials in biomedicine: Precision drug delivery and cancer therapy. International Journal of Biological Macromolecules. 2024; 130746.
[69] Pei JJ, Yan Y, Palanisamy CP, Jayaraman S, Natarajan PM, Umapathy VR, Gopathy S, Roy JR, Sadagopan JC, Thalamati D, Mironescu M. Materials-based drug delivery approaches: Recent advances and future perspectives. Green Processing and Synthesis. 2024; 13: 20230094.
[70] Pei JJ, Deng W, Liu Y, Guo Y, Chen J, Abdu H, Khan MR, Palanisamy CP, El-Aty AM. A Comprehensive Review of Cornus officinalis: Health Benefits, Phytochemistry, and Pharmacological Effects for Functional Drug and Food Development. Frontiers in Nutrition. 2023; 10: 1309963.
[71] Alugoju P, Palanisamy CP, Anthikapalli NVA, Jayaraman S, Prasanskulab A, Chuchawankul S, Dyavaiah M, Tencomnao T. Exploring the anti-aging potential of natural products and plant extracts in budding yeast Saccharomyces cerevisiae: A review. F1000Research. 2023; 12: 1265.
[72] Lavanya M, Krishnamoorthy R, Alshuniaber MA, Manoharadas S, Palanisamy CP, Veeraraghavan VP, Jayaraman S, Rajagopal P, Padmini R. Formulation, characterization and evaluation of gelatin-syringic acid/zinc oxide nanocomposite for its effective anticancer, antioxidant and anti-inflammatory activities. Journal of King Saud University-Science. 2023; 35: 102909.
[73] Palanisamy CP, Poompradub S, Sansanaphongpricha K, Jayaraman S, Subramani K, Sonsudin F. Biosynthesis of silver nanoparticles (AgNPs) using ethanolic extract of Nigella sativa (L.) seeds promotes wound healing via PDGF and VEGF signalling pathways activation. Biocatalysis and Agricultural Biotechnology. 2023; 54: 102970.
[74] Prasad M, Jayaraman S, Natarajan SR, Veeraraghavan VP, Krishnamoorthy R, Gatasheh MK, Palanisamy CP, Elrobh M. Piperine modulates IR/Akt/GLUT4 pathways to mitigate insulin resistance: Evidence from animal and computational studies. International Journal of Biological Macromolecules. 2023; 253: 127242.
[75] Palanisamy CP, Pei JJ, Phaniendra A, Venkata AAN, Jayaraman S, Veeraragahavan VP, Sridevi G, Roy JR, Janaki CS, Thalamati D, Mironescu M, Luo Q, Chai Y, Long Q. New Strategy of Neurodegenerative Disease Treatment with Extracellular Vesicles (EVs) Derived from Mesenchymal Stem Cells (MSCs). *Theranostics*. 2023; 13(12):4138-4165. doi:10.7150/thno.83066.
[76] Palanisamy CP, Phaniendra A, Jayaraman S, Poompradub S. *Nigella sativa* L. seed extracts promotes wound healing progress by activating VEGF and PDGF signalling pathways: *An in vitro* and *in silico* study. *F1000 Research*. 2023; 12: 436.
[77] Pei JJ, Palanisamy CP, Phaniendra A, Venkata AAN, Natarajan PM, Umapathy VR, Swamikannu B, Jayaraman S, Rajagopal P, Poompradub S. A comprehensive review on bio-based materials for chronic diabetic wounds. *Molecules*. 2022; 28(2), 604.